1 **Title**

2

3 Neural subspaces of imagined movements in parietal cortex remain stable over several years in humans.

4

5 **Authors and Affiliations**

6

7 Bashford L[1*], Rosenthal I[1], Kellis S[1], Bjånes D[1], Pejsa K[1], Brunton BW[2] and Andersen RA[1]

8

9 *Corresponding Author: bashford@caltech.edu

10 1. Division of Biology and Biological Engineering, and T&C Chen Brain-Machine Interface Center,

11 California Institute of Technology, Pasadena, CA, USA.

12 2. Department of Biology, University of Washington, Seattle, WA, USA.

13

14 **Abstract**

15

16 A crucial goal in brain-machine interfacing is long-term stability of neural decoding performance, ideally

17 without regular retraining. Here we demonstrate stable neural decoding over several years in two

18 human participants, achieved by latent subspace alignment of multi-unit intracortical recordings in

19 posterior parietal cortex. These results can be practically applied to significantly expand the longevity

20 and generalizability of future movement decoding devices.

21

22 **Main Text**

23

24 Brain-machine interfaces (BMIs) decode neural activity to reproduce the user's intention and assist

25 individuals with physical and neurological disabilities. In motor BMIs, the user commonly imagines or

26 attempts to make a movement, and the corresponding recorded neural activity is decoded to guide

27 movement in the intended direction, either on a computer or a prosthetic [1,2]. BMIs can use neural

28 signals acquired at different spatial and temporal resolution, but these have tradeoffs in performance

29 and stability. Whereas single- or multi-unit recordings provide the highest information content, these

30 recordings suffer from non-stationarity – different individual neurons are recorded from day to day or

31 even morning to afternoon[3,4]. This variation is caused by several factors, including movement of the

32 electrodes, changes in the electrode-tissue interface, and degradation of the electrodes. Thus, as the

33 neural features used to train the decoder change, the performance of the BMI degrades over time. As

34 BMIs are implanted for increasingly long durations [5,6] the longitudinal stability of intracortically recorded

35 neural activity is a central challenge to the practical utility of BMI devices. Currently, long-term use of

36 BMI devices is only possible when users perform frequent retraining, often several times in a single day,

37 to maintain desired performance. In addition to being time consuming, frequent retraining may not be

38 possible in some use cases, for example in degenerative diseases (e.g., ALS/MND – amyotrophic lateral

39 sclerosis/motor neuron disease) where the loss of function over time may eventually prevent the

40 performance of training tasks.

41

42 Although different neurons from the same population are being recorded, the lower-dimensional

43 subspaces of the neural dynamics may remain relatively stable [7,8]; we investigate this intriguing

44 possibility in the context of BMI decoding. Alternative neural signals such as the local field potential

45 have been observed to be more stable over time [9,10]; however, the tradeoff is a reduction in information

46   content compared to single unit activity, which ultimately limits decoding performance. Therefore, the

47   most promising solution currently being investigated is to use 'latent signals' for BMIs. Latent signals are

48   derived from low-dimensional subspaces of the original high-dimensional single- or multi-unit (MUA)

49   neural activity, and they have been shown to preserve information content while minimizing non-

50   stationarity [11–15]. Most stable latent spaces have so far been identified and validated primarily in

51   longitudinal recordings of non-human primate primary sensorimotor cortices. In this paper, we

52   investigate the potential of these latent signals for BMI control in two human participants, for whom

53   neural signals were recorded in higher order cortical areas over several years [16,17]. Specifically, we

54   demonstrate that the neural subspace of imagined reaches in a center-out task remained remarkably

55   stable in posterior parietal cortex.

56

57   Data were collected on 143 and 73 unique days, aggregated over a total period of 1106 and 871 days,

58   for participant 1 [1] and 2 [18], respectively. Participant 1 attempted reaches in 4 directions while MUA was

59   recorded from Brodmann Area 5 (BA5) and the Anterior Intraparietal Area (AIP). Participant 2 attempted

60   reaches in 8 directions while MUA was recorded from the junction of the postcentral and intraparietal

61   sulcus (PC-IP) (Fig. 1A). We use only the 'training' trials for longitudinal analysis, without any decoder

62   present, to ensure the data were directly comparable from day-to-day [19]. During these trials,

63   participants imagined moving their arm to follow the movement of an on-screen cursor. To process the

64   neural data, we adapted methods established in non-human primates [12]. First a latent signal for each

65   day on which the experiment occurred is calculated by performing Principal Component Analysis (PCA) [7]

66   on all trials that day. The latent signal is then aligned for all pairs of days using Canonical Correlation

67   Analysis (CCA) [20]. A Linear Discriminant Analysis (LDA) was used to classify the target locations (Fig. 1B).

68   An LDA model was trained using data from Day N and tested within day (N on N) using leave one out

69   cross validation (LOOCV). This analysis was then repeated for every possible pair of training day N and

70   testing day M. Further materials and methods information can be found in the 'Methods' section of this

71   manuscript.

72

73   When decoding the MUA signal, we observe good decoding accuracy (Fig. 2A, MUA – red) within the

74   same day, but this accuracy quickly degrades as the number of days between training and testing day

75   increases (Fig. 2A, MUA – black). Intriguingly, aligned latent neural activity space substantially improves

76   the accuracy (Fig. 2A, Latent). In particular, across all pairs of days, the decoding performance that can

77   be achieved is higher from the latent signal (mean±SD, AIP: 51.2±8.38%, BA5: 63.7±12.0% and PCIP:

78   45.8±8.63%) than that achieved with MUA (mean±SD, AIP: 35.4±11.1%, BA5: 34.6±12.1% and PCIP:

79   25.5±11.8%) (all differences $p<0.001$, Wilcoxon Sign Rank test, Bonferroni corrected) (Fig. 2B). Further,

80   the across-day training produces a comparable performance compared to within-day using aligned

81   latent data. Across all recording electrode arrays, the correlation between performance and time

82   between the pairs is smaller for latent signals (AIP $r = -0.066$, BA5 $r = 0.020$, PCIP $= -0.033$, Pearson's

83   linear correlation coefficient) than for MUA (AIP $r = -0.12$, BA5 $r = -0.30$ PCIP $r = -0.29$, Pearson's linear

84   correlation coefficient). To summarize these results, we calculate the ratio of performance between all

85   the within-day models and all the across-day models for latent and MUA activity. A ratio of 1 represents

86   a comparable result, a value greater than one would mean that across-day pairs performed better than

87   within-day pairs and vice versa for values below 1 (Fig. 2C). Here we see that in all cases the ratio of

88   latent signals is higher than MUA demonstrating the aligned latent signal across days has significantly

89   increased stability compared to the MUA activity ($p<0.001$, Wilcoxon signed rank test, Bonferroni

90   corrected. Participant 1 N = 20449, Participant 2 N = 5329).

91

92   In this task, the participants were not required to learn anything novel, so we do not expect neural

93   activity changes related to learning. However, the repetitive nature of the task and the amount of time

94   spent performing it may still alter the brain activity representing the task over time. To investigate the

95   way in which the task is represented in the latent signal over time, we calculated the Principal Subspace

96   Angle (PSA) [21,22] between all pairs of days (Fig. 3A). This angle reflects the magnitude to which the

97   subspaces in the pair must be rotated to be maximally correlated, which is one way to measure the

98   extent to which CCA rotates the latent neural data to align day pairs [23]. A smaller PSA indicates a more

99   similar representation between pairs. We computed the first PSA in participant 1 only, who had two

100 arrays in different functional areas. We controlled for changes in the health of the array, which were not

101 significantly different for the two arrays over time (see Methods Fig. 1C). We divided up the data into

102 early and late periods (Methods Fig. 1A), where late was defined as the resumption of the experiment

103 after a significant break (akin to a 'washout' in the familiarity of the task). Over all pairs of days, the

104 variability in PSA in BA5 was smaller than for AIP (Fig. 3B left column). We then focused on close pairs of

105 days within the early and late phases of data collection, those with a difference of only up to 10 days

106 (Fig. 3B right column). Interestingly, after the break in the experiment, we find a significant difference in

107 the representation of the data across these relatively close day pairs in only area AIP and not area BA5

108 (p<0.001, Wilcoxon Signed Rank Test). This finding indicates a more stable intrinsic representation of

109 reaching in area BA5 than AIP.

110

111 Here we have demonstrated the stable representation of neural activity in subspaces of human

112 intracortical recordings over several years. This result validates methods of aligning latent spaces

113 developed in non-human primates during actual reaching [12,24,25], here applied successfully in imagined

114 reaches by humans. Furthermore, we have extended the finding of stable subspaces beyond the primary

115 sensorimotor cortices into higher-order association areas in humans. The aligned latent signal performs

116 best in decoding overall in each site, but the magnitude of the improvement reduces as the recordings

117 come from more cognitive brain regions. We see the same effect in the PSA, where the variability in

118   representation increased in the more cognitive brain region. We hypothesize that this trend is due to an

119   increased flexibility in neuronal processing facilitating higher order/conceptual aspects of reaches (in

120   AIP) compared to a more fundamentally engrained processing in the lower order sensorimotor control

121   of a limb (in BA5).

122

123   There are few human intracortical BMI datasets available to validate the performance of latent signals

124   over substantial periods of time in the same task. Participants enrolled in intracortical clinical trials are

125   typically encouraged to perform a much broader range of tasks, with each requiring little to no training.

126   Consequently, far fewer trials are available for any specific experimental paradigm. Chronic experiments

127   exploring the human cortex offer a unique opportunity to study various changes in neural circuits over

128   extended periods of time. Based on our results, we encourage the design of future studies to facilitate

129   longitudinal task data collection and data collection from cortical sites beyond the traditionally used

130   primary motor and sensory cortices. As we show here, these data allow the identification and validation

131   of stable neural features which enable the long-term use of BMIs without the need for retraining, thus

132   paving the way for BMIs to be used in many more cases; by individuals who lose the ability to retrain

133   due to degenerative condition, or those who suffer injuries that preclude electrode implants in primary

134   sensorimotor cortex. With the identification of such robust features, one promising direction for future

135   work may be to enable the development of generalized BMIs that can be trained on data from

136   individuals other than the eventual intended user [26].
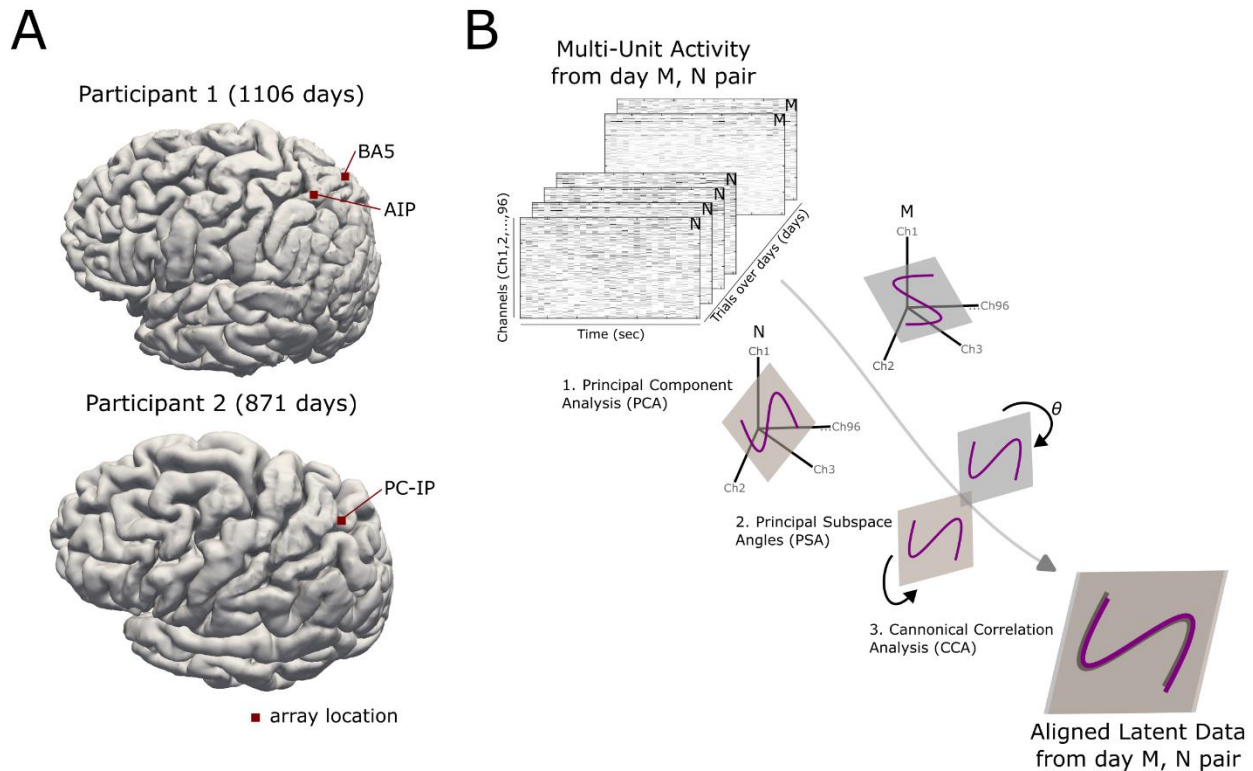
137

138

139

140   **Figures**

141

142

143

144   Figure 1. Methods. A) The neural signal was recorded on all days of the task using the same

145   microelectrode arrays (Blackrock Neurotech). Arrays were implanted in the Anterior Intraparietal Area

146   (AIP) and Brodmann Area 5 (BA5) of participant 1, and the junction of the postcentral and intraparietal

147   sulcus (PC-IP) in participant 2. B) Data were arranged in a tensor of multi-unit activity (MUA) on each

148   channel, of each trial completed during the duration of the study. All trials within a day were grouped

149   and a pair of days was selected for further analysis (e.g., day N or M). For each day, the latent neural

150   data was calculated using principal component analysis (PCA). The latent data were aligned by canonical

151   correlation analysis (CCA), and the magnitude of the alignment was calculated as the principal subspace
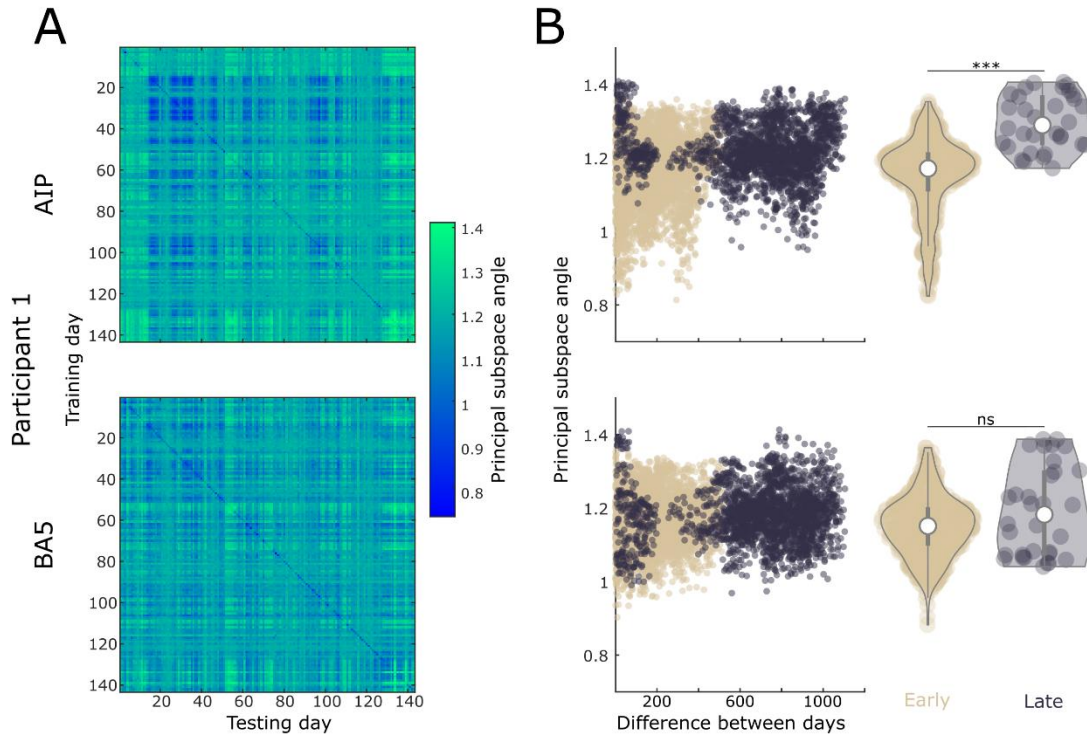
152   angle (PSA).

153
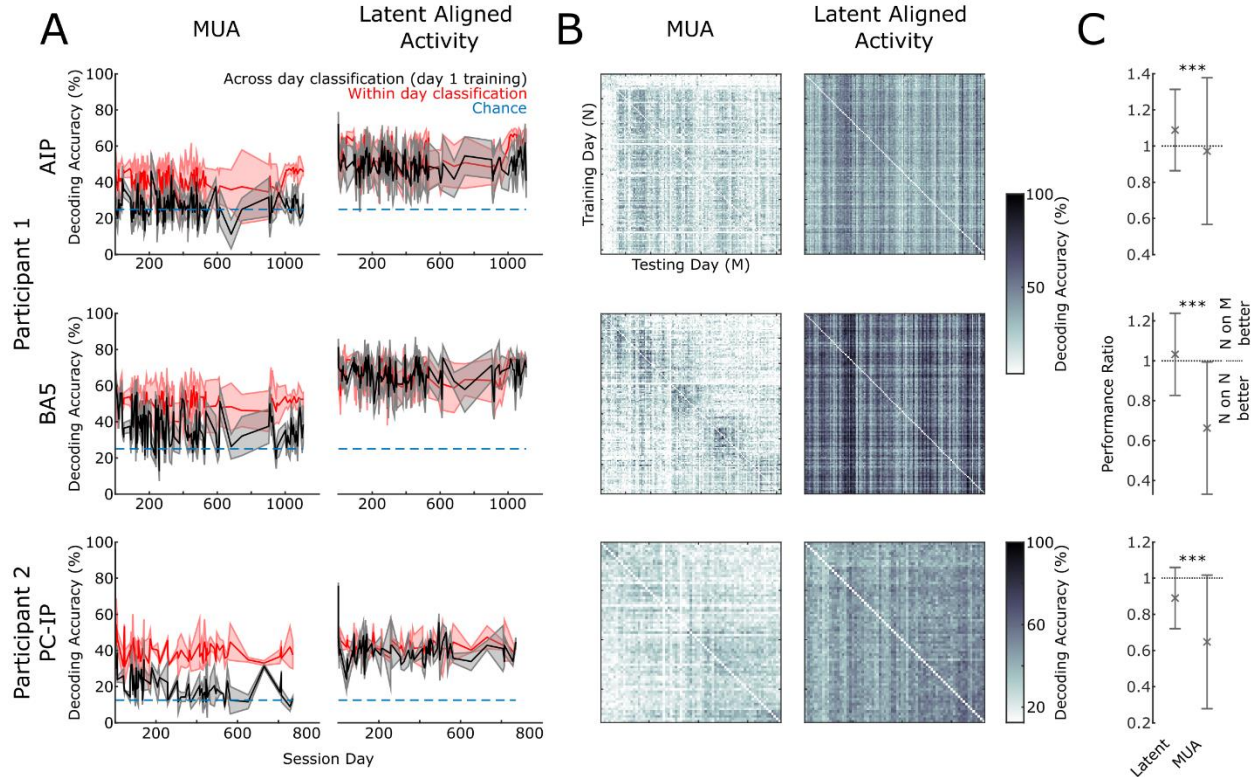
Figure 2. Classification decoder accuracy for two human participants. A) Left column: the performance of the LDA classifier using the raw multi-unit activity (MUA) from the brain regions AIP (top), BA5 and PCIP (bottom). The red line shows the classification accuracy when the data from the same day (N on N) is used for training and testing with leave-one-out cross validation. The black line shows the classification accuracy when data from session day N is used for testing, but training is always performed on data from a single day (in this example day 1). Shading shows the standard deviation, dotted line shows the chance level for classifications. Right column: the same analysis as the left column but using the latent aligned data. B) The decoding accuracy of every pair of days for MUA and Latent activity. C) The ratio of performance between within day and across day decoding, error bars show standard deviations, stars indicate significance.

Figure 3. Principal subspace angles. A) The principal subspace angle (PSA) calculated between all pairs of days for AIP (top) and BA5 (bottom). B) Left Column: the PSA between each pair of days, colored according to the early and late period (Methods Fig 1A.) Right Column: violin plots of only the day pairs where the difference between days is 10 or less, grouped into the early and late period.

175   **Methods**

176

177   All procedures were approved by the Internal Review Boards of California Institute of Technology,

178   University of Southern California, Rancho Los Amigos National Rehabilitation Center, University of

179   California Los Angeles and Casa Colina Hospital and Centers for Healthcare. Informed consent was

180   obtained from all participants after the nature of the study and possible risks were explained. This work

181   was performed as part of Clinical Trials: NCT01849822, NCT01958086, NCT01964261.

182

183   *Participants*

184

185   Participant 1 was a 32-year-old tetraplegic male at the time of implantation. He was implanted with two

186   microelectrode arrays on 17 April 2013. The electrodes were implanted in Brodmann Area 5 (BA5) and

187   the Anterior Intraparietal Area (AIP). He had a complete lesion of the spinal cord at cervical level C3-4,

188   sustained 10 years earlier, with paralysis of all limbs. Participant 2 was a 59-year-old tetraplegic female

189   at the time of implantation. She was implanted with two arrays but only one was used in this study, at

190   the junction of the post-central and intraparietal gyrus (PC-IP) on 29 August 2014. The other array was

191   not functional. She had a C3-C4 spinal lesion (motor complete) sustained 7 years earlier, and retained

192   movement and sensation in her upper trapezius, without control or sensation in her hands. During their

193   enrollment, the participants performed many different tasks. The data for the analysis presented in this

194   manuscript were collected on 143 and 73 unique days, over a period of 1106 and 871 days, for

195   participant 1 and 2, respectively.

196

197   *Task and Data Collection*

198

199   The center out task was intended to allow the participants to spatially position a cursor on a computer

200   screen. Targets were presented one at a time on the LCD display. The LCD monitor was positioned

201   approximately 184cm from the subject's eyes. Stimulus presentation was controlled using the

202   Psychophysics Toolbox for MATLAB. During recording-only sessions, without any decoder, a circular

203   cursor on the screen would move automatically from the center to one of either 4 (participant 1) or 8

204   (participant 2) targets arranged radially around the center point. Following a 250ms delay relative to

205   target onset, the cursor moved in a straight line directly to the target with an approximately bell-shaped

206   velocity profile. Each trial lasted 3 seconds. The number of trials completed by the participants on each

207   day during the study is shown in Methods Fig. 1A and B. Participants were asked to imagine making

208   movements of the arm to mimic the movements observed on the screen.

209

210   The NeuroPort System (Blackrock Neurotech, UT, USA), comprising the arrays and neural signal

211   processor (NSP), has received Food and Drug Administration (FDA) clearance for <30 days of acute

212   recordings. For this study we received FDA IDE (Investigational Device Exemption) clearance for

213   extending the duration of the implant. The health and performance of the arrays was assessed as the

214   mean impedance across all electrodes on each array, recorded on each day of the experiment.

215   Impedance data is available for participant 1 only (Methods Fig. 1C). Multi-Unit Neural Activity (MUA)

216   was amplified, digitized, and recorded at 30 kHz with the NeuroPort NSP. The threshold for calculation

217   of MUA spikes was -3.5 * root mean squared voltage, calculated over each recording session. Data was

218   organized into a three-dimensional tensor; The first dimension was the MUA binned into non-

219   overlapping 50ms windows. The second dimension was the number of electrodes (96 for each array).

220   The third dimension was the index of trials ordered chronologically from the first to last over the entire

221   study period.

222

223   *Analysis*

224

225   The analysis methods used in this manuscript extend the analysis of Gallego and colleagues [12] who

226   demonstrated success in long-term decoding from primate motor cortex recordings. Data from each

227   participant and each array was processed separately. The analysis was completed identically between all

228   pairs of all days in which the participants completed the center out task. For the following description of

229   the analysis two such days are represented as day M and day N.

230

231   Initially the same number of trials, containing equal presentation of all targets, are taken on each day.

232   On days with different numbers of trials, we used all the trials on the day with the fewer trials and then

233   randomly selected the same number of trials from the other day. To ensure all the trials for a pair of

234   days were used, the entire analysis was repeated 1000 times, each iteration using a different randomly

235   selected set of trials. All electrodes (96) and all time bins were included for all trials. For each day this

236   produced a (electrode x time x trials) matrix. The data was concatenated across trials and then

237   dimensionality reduction was performed using Principal Components Analysis (PCA) ('pca' function,

238   Matlab 2021b). We reduced the data to 10 dimensions, following previous analysis, but confirmed that

239   the results did not qualitatively change using a larger range of values. The result of the PCA analysis was

240   a (10 x time*trials) matrix. We call this the 'latent data'. The latent data from each day in the pair was

241   then aligned using Canonical Correlations Analysis (CCA) ('canoncorr' function, Matlab 2021b). This

242   produced a (10 x time*trials) matrix. We call this the 'aligned latent data'. The data was then split back

243   into individual trials (10 x time x trials) and the activity in each trial ('time' dimension) was averaged

244   producing a (10 x 1 x trials) matrix for each day M and N. This was then used to calculate a linear

245   regression model for classification ('fitlm' function, Matlab 2021b). The aligned latent data were used as

246   the data and the target labels for each trial were used as the model. For within day calculations of

247   classification accuracy a leave-one-out cross validation (LOOCV) was used to calculate classification

248   accuracy. For calculating classification accuracy across days, the entire data from day M was used to

249   train the LDA model, which was tested on the entire dataset from day N (and vice versa). To calculate

250   the Principal Subspace Angle (PSA) we followed the method presented by Knyazev and colleagues [21]

251   ('subspacea' function, MATLAB Central File Exchange, Matlab 2021b). We present data from the first

252   PSA, but we note the results remained qualitatively consistent when summing over all PSAs calculated

253   from the data.

254   We only perform the PSA analysis on participant 1 because two electrode locations were recorded. In

255   this case AIP and BA5 control for each other in factors related to changes in electrode-tissue interface

256   that could influence the results (see Methods Figure 1C). We assume that since this crucial metric is

257   consistent between the two arrays analytical differences can be explained by the different

258   neurophysiology of the regions. Since there is only the PCIP array in participant 2 we cannot make the

259   same assumption about differences over time, as without a comparison, analytical differences may be

260   due to changes in the electrode-tissue interface.

261

262   Data availability
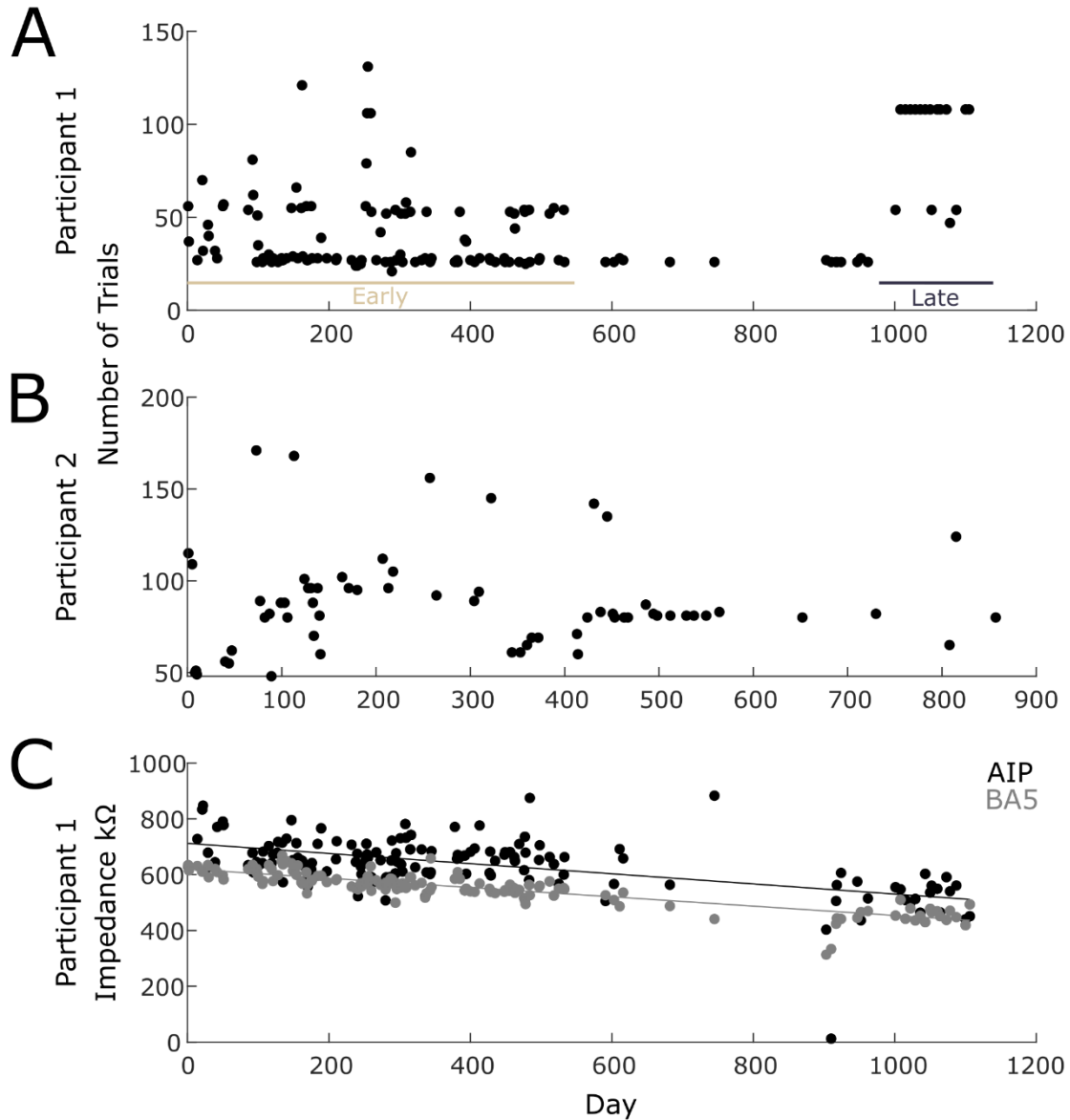
263

264   The datasets analyzed for this manuscript will be shared upon reasonable request.

265

266   Code availability

267

268   All analyses were implemented using custom Matlab (The Mathworks Inc.) code. Code to replicate the

269   main results will be shared upon reasonable request.

270

Methods Figure 1. Data collection. A & B) Varying numbers of trials of the same task were collected on each day. Participant 1 only – during a middle period relatively few trials of the task were performed to focus on other experiments. Data collected were split into an 'Early' and 'Late' period. C) The impedance of each array on each day experiments were collected. Impedance data are only available for participant 1.

286 **References**

287

288 1. Aflalo, T. et al. *Science* **348**, 906–910 (2015).

289 2. Hochberg, L.R. et al. *Nature* **442**, 164–171 (2006).

290 3. Dickey, A.S., Suminski, A., Amit, Y. & Hatsopoulos, N.G. *J. Neurophysiol.* **102**, 1331–1339 (2009).

291 4. Stevenson, I.H. et al. *J. Neurophysiol.* **106**, 764–774 (2011).

292 5. Simeral, J.D., Kim, S.-P., Black, M.J., Donoghue, J.P. & Hochberg, L.R. *J. Neural Eng.* **8**, 025027 (2011).

293 6. Hughes, C.L. et al. *J. Neural Eng.* **18**, 045012 (2021).

294 7. Cunningham, J.P. & Yu, B.M. *Nat. Neurosci.* **17**, 1500–1509 (2014).

295 8. Williamson, R.C., Doiron, B., Smith, M.A. & Yu, B.M. *Curr. Opin. Neurobiol.* **55**, 40–47 (2019).

296 9. Flint, R.D., Wright, Z.A., Scheid, M.R. & Slutzky, M.W. *J. Neural Eng.* **10**, 056005 (2013).

297 10. Flint, R.D., Scheid, M.R., Wright, Z.A., Solla, S.A. & Slutzky, M.W. *J. Neurosci.* **36**, 3623–3632

298 (2016).

299 11. Pandarinath, C. et al. *Nat. Methods* **15**, 805 (2018).

300   12.   Gallego, J.A., Perich, M.G., Chowdhury, R.H., Solla, S.A. & Miller, L.E. *Nat. Neurosci.* **23**, 260–270

301   (2020).

302   13.   Natraj, N., Silversmith, D.B., Chang, E.F. & Ganguly, K. *Neuron* **110**, 154-174.e12 (2022).

303   14.   Trautmann, E.M. et al. *Neuron* **103**, 292-308.e4 (2019).

304   15.   Elsayed, G.F. & Cunningham, J.P. *Nat. Neurosci.* **20**, 1310–1318 (2017).

305   16.   Andersen, R.A., Aflalo, T., Bashford, L., Bjånes, D. & Kellis, S. *Annu. Rev. Psychol.* **73**, 131–158

306   (2022).

307   17.   Gallego, J.A., Makin, T.R. & McDougle, S.D. *Trends Neurosci.* **45**, 176–183 (2022).

308   18.   Aflalo, T. et al. *Sci. Adv.* **6**, eabb3984 (2020).

309   19.   Orsborn, A. & Carmena, J.M. *Front. Comput. Neurosci.* **7**, 157 (2013).

310   20.   Bach, F.R. & Jordan, M.I. *J. Mach. Learn. Res.* **3**, 1–48 (2003).

311   21.   Knyazev, A.V. & Argentati, M.E. *SIAM J. Sci. Comput.* **23**, 2008–2040 (2002).

312   22.   Björck, Åke & Golub, G.H. *Math. Comput.* **27**, 579–594 (1973).

313   23.   Williams, A.H., Kunz, E., Kornblith, S. & Linderman, S. *Adv. Neural Inf. Process. Syst.* **34**, 4738–

314   4750 (2021).

315   24.   Degenhart, A.D. et al. *Nat. Biomed. Eng.* **4**, 672–685 (2020).

316   25.   Karpowicz, B.M. et al.2022.04.06.487388 (2022).doi:10.1101/2022.04.06.487388

317   26.   Peterson, S.M., Steine-Hanson, Z., Davis, N., Rao, R.P.N. & Brunton, B.W. *J. Neural Eng.* **18**,

318   026014 (2021).

319

320

321